Vertical Scales of Turbulence at the Mt. Wilson Observatory

Robert N. Treuhaft and Stephen T. Lowe
Jet Propulsion Laboratory, California Institute of Technology, Pasadena, California 91109

and

Manfred Bester, William C. Danchi,
and Charles H, Townes
Space Sciences Laboratory, University of California at Berkeley, Berkeley, California *94720*

ABSTRACT

The vertical scales of turbulence at the Mt. Wilson observatory are inferred from data from the University of California at Berkeley Infrared Spatial Interferometer (1S1), by modeling path length fluctuations observed in the interferometric paths to celestial objects and those in instrumental ground-based paths. The correlations between the stellar and ground-based path length fluctuations and the temporal statistics of those fluctuations are modeled on various time scales to constrain the vertical scales. A Kolmogorov-Taylor turbulence model with a finite outer scale was used to simulate 1S1 data. The simulation also included the white thermal noise of the interferometer, aperture filtering effects, and the data analysis algorithms. The simulations suggest that the path delay fluctuations observed in the 1992-3 1S1 data are largely consistent with being generated by refractivity fluctuations at two characteristic vertical scales: one extending to a height of 45 m above the ground, with a wind speed of about 1 m/see, and another at a much higher altitude, with a wind speed of about 10 m/see. The height of the lower layer is of the order of the height of trees and other structures near the interferometer, which suggests that these objects, including elements of the interferometer, may be responsible for generating the lower layer of turbulence. The modeling suggests that the high-altitude component contributes primarily to short-period ($<$ 10 seconds) fluctuations, while the lower component dominates the long-period (up to a few minutes) fluctuations. Simulations further show that there is the potential for improving the seeing or astrometric accuracy by about 30-50910 on average, if the path length fluctuations in the lower component are directly calibrated. Statistical and systematic effects induce an error of about 15 m in the estimate of the lower component turbulent altitude.

Subject headings: turbulent atmospheric height, interferometry, astrometry

1. Introduction

The spatial scales of atmospheric turbulence at an astronomical site are important for devising techniques for minimization of turbulence effects, as well as for understanding the dynamics of turbulence generation. The lateral spatial scales of refractivity fluctuations are related to the temporal scales through the Taylor hypothesis of frozen flow, and they therefore affect both the time dependence of interferometric phase statistics and their baseline dependence. The vertical scales of turbulence, which are the primary subject of this paper, also affect the dependence of interferometric phase on time and baseline length. For example, the height of the turbulent atmosphere affects the power law dependence of the phase structure function on baseline length (Treuhaft and Lanyi 1987). The vertical scales of the turbulent atmosphere are also an important input to the design of calibration strategies aimed at reducing the effect of turbulence on interferometric phase, which is used in astrometry. In this paper, the vertical scales of turbulence on Mt. Wilson are inferred from the University of California at Berkeley Infrared Spatial Interferometer (1S1) data, using the correlations between path length fluctuations along stellar paths with those along ground-based paths within the 1S1. The statistics of the fluctuations on the stellar and ground-based paths taken separately are also used to determine the vertical scales.

Qualitatively, high correlations between stellar and ground-based path length fluctuations suggest contributions from low-lying atmospheric components. While low turbulent altitudes increase the measured correlation, thermal noise in the interferometer and spatial filtering of short-period stellar path length fluctuations, due to the dimensions of the 1S1 apertures, both tend to decrease the correlation. If, in addition to low-lying turbulent components, a high-altitude component is also postulated, its effect will also be to decrease the stellar/ground-based path length correlation. The above effects each contribute to the temporal statistics of the stellar and ground-based fluctuations, and the temporal statistics of the observed and modeled fluctuations must therefore be considered. In the next section, the 1S1 data will be described. Section 3 contains a general description of the process of inferring vertical scales from the data, and section 4 presents the quantitative modeling and simulation used to infer turbulent altitudes from the observed correlations and temporal statistics. Section 5 discusses the results of the modeling and simulation of section 4 and assigns error levels to the atmospheric parameters inferred from the data. Section 6 discusses improvements to the current approach and plans for further investigations into the vertical scales of turbulence at Mt. Wilson.

2. Experimental Equipment and the Data Obtained

Figure 1 shows a single trailer of the 1S1, which contains one of the two telescopes used in the interferometer. The stellar infrared radiation is reflected from the steerable flat mirror on the right and then focused by the parabolic mirror on the left through a central hole in the flat mirror to the optics table behind the flat mirror. A helium-neon laser distance interferometer (LDI) monitors the electromagnetic path length from the parabola to a cat's eye at the center of rotation of the flat mirror, and another LDI the path length from the parabola through the central hole in the flat mirror to a

focal point on the optics table. The total length of the LDI paths, from the flat mirror, to the parabolic mirror, and back through the flat mirror to the optics table, is about 11 m. A more detailed discussion of the system can be found in Bester et al. (1992).

An 1S1 path length fluctuation time series, for an observation of the star Alpha Orionis, is shown in infrared cycles (11. 15μm) in Figure 2, along with the telescope-differenced LDI data for a 6-minute observation. Stellar path length data, which include atmospheric path length fluctuations as well as those along the ground-based paths measured by the LDIs (Figure 1), will be called "IR" data. The IR data in Figure 2 were taken on 8 September 1992 on a 13-m baseline. A constant slope has been removed from both the IR and LDI data, because errors in the telescope geometry, assumed in the interferometric cross-correlation of the signals from the two telescopes, could introduce a slope in the IR data which would not be present in the LDI data. The IR phase has been determined from averages over a time of 0.2 seconds. The LDI phase is read out every 0.1 second. There is a clear correlation between the IR and LDI time series but there may also be cycle slips, for example between 678 and 679 minutes. Cycle assignments for the IR data were made so that no two adjacent points would differ by more than 0.5 IR cycles. The LDI data are free of cycle slips because the signal to noise ratio is very large, and the response time of the LDI circuitry is much less than one millisecond. It is also clear from Figure 2 that cycle slips may affect the correlation between the IR and LDI data. The IR data exhibit larger path length fluctuations, with an rms of 0.63 IR cycles, than do those from the LDI, with an rms of 0.18 IR cycles. The IR-LDI correlation of the data of Figure 2 is about 0.5.

Figure 2 represents a scan for which cycles were reasonably well connected, but in examining all the 1S1 phase data from 1992 and 1993, it was clear that, for many scans, frequent cycle slips could affect the IR-LDI correlation. The following data-editing method was used to subdivide scans into nearly cycle-slip-free sections: For each scan, point-to point cycle jumps with magnitudes greater than 1/3 cycle were identified and the data were cut into intervals between those jumps; correlations were evaluated within the cut intervals. Thus, within the selected intervals, there are no adjacent points with phase jumps between 1/3 and 1/2 cycle, and there will also be no jumps with magnitudes between 1/2 and 2/3 cycles, which alias back into the 1/3- to 1/2-cycle range. The data intervals chosen in this way can only contain point-to-point changes in the range of -1/3 to 1/3 cycle and jumps of magnitude 2/3 cycle and greater. Figure 3 shows a histogram of the point-to-point phase changes for the data of Figure 2, for which a 0.2-second integration time was used. It can be seen that there are very few point-to-point changes as large as 0.4-cycles, and it is therefore a safe assumption that there are almost no changes greater than 2/3 cycles. Limiting individual time scales for data to ones with maximum apparent phase change of 1/3 cycle greatly reduces cycle slips in the analyzed data.

Figure 4a shows the average correlation for intervals cut as described above, versus interval duration given on the abscissa. The error bars are the standard deviation of the mean (standard deviation of the correlations in the time bin divided by the square root of the number of samples in that bin) for the given interval. The average correlation in Figure 4a is about 0.45 for the longer time intervals, going down to about 0.2 for the shortest intervals. Figure 4b shows a histogram of the number of cut intervals as a function of their length. If the probability per unit time of a phase jump of magnitude 1/3 cycle or greater were fixed, Figure 4b would be proportional to the exponential Poisson

probability for finding no such jumps in the interval indicated on the abscissa. The fact that the histogram is not well-represented by an exponential is an indicator that it is generated by a mixture of levels of phase fluctuation, which will be discussed in section 4. The figures are derived from all 1S1 observations of Alpha Orionis taken in 1992 and 1993, for which there were both IR and LDI data. Due to the longer baselines of 10-13 ml other sources, for which phase is obtainable on shorter baselines, were resolved and were not useful in this study. In the future, shorter baselines of 4 m could be used to extend the number of sources available for 1S1 phase measurements. The physical mechanisms which could potentially generate Figure 4 will be discussed in section 4.

3. Inferring Turbulent Altitudes from IR and LDI Data

In this section, we give an overview of the turbulent altitude[1] information contained in 1S1 data. It was noted by Bester et al. (1992) that LDI measurements within the two telescopes showed closely correlated fluctuations, and also that the IR path length fluctuations were frequently highly correlated with those measured within the instrumental paths of the 1S1 with LDIs, difference between telescopes, as in Figure 2. This implies either that mechanical fluctuations dominate the interferometric stochastic signatures, or that atmospheric fluctuations close to the ground comprise an appreciable part of the total atmospheric turbulence effects, suggesting rather large fluctuations within a low turbulent atmospheric height. Mechanical fluctuations are largely ruled out, because there is no known mechanism which would produce mechanical fluctuations at the observed, several-micron level between two telescopes separated by $\approx 10m$. In addition, fluctuations in the IR path, which are correlated with those in the telescope-differenced LDI paths, are frequently 2-3 times greater in magnitude and hence must occur over distances which are larger than the LDI paths, i.e., which are outside the telescopes. The LDI fluctuations in Figure 2 represent the difference between the two LDI paths within each of the two telescopes, which is essentially the same path traveled, within the telescopes, by the IR radiation, Figure 2 shows that not only are many of the larger fluctuations correlated between the IR and LDIs, but that the former tend to be $\approx$ 2-3 times larger than the latter. This immediately indicates that the same fluctuations that occur in the LDI paths extend above the telescope for $\approx$ 20 meters of the IR path.

Another qualitative argument for extension some distance above the telescopes of the perturbations seen by the LDIs can be made from their horizontal extent. The larger fluctuations last for times in the range of 10-30 seconds. If the wind speed near the ground is about 1 m/see, then the horizontal dimensions of these larger fluctuations are 10-30 m. This same size is demonstrated by notable correlations between the LDI fluctuations of the two telescopes, even when they are separated by 10 m or more. Hence, if the vertical spatial extent of refractivity fluctuations is of the order of their horizontal extent, as in 3-dimensional Kolmogorov-type turbulence, perturbations are expected to extend of the order of 10-30 meters above the ground.

---

[1] Throughout this paper, "altitude" means the height of the top of the turbulent layer, or the thickness of the layer.

In order to quantitatively estimate the vertical scales of turbulence from the data, calculations of the correlation between the IR path length fluctuations and those along the LDI paths were performed, based on a Kolmogorov-Taylor model (Treuhaft and Lanyi, 1987) with a finite outer scale. The statistics of fluctuations along the IR and LDI paths taken separately were also modeled and compared to the 1S1 data to constrain the possible vertical scales allowed by the IR-LDI correlation alone. The effect of cycle slips in the IR data was minimized with the data-editing technique described in the previous section. Simulated data, including atmospheric fluctuations, thermal noise contributions, and the finite-aperture filtering effects to be described in subsection 4b, were processed with these data-editing techniques, and the resulting IR-LDI correlations and temporal statistics compared to those of the real data taken in the 1992 and 1993 observing seasons.

As will be discussed in subsection 4b, it was found that the IR-LDI correlation, and the short- and long-term IR and LDI fluctuation levels, could not be modeled by a single turbulent layer with one height. Key features of the data were simulated with turbulence arising over two characteristic altitudes, one at about 45 m, over which fluctuations are correlated with LDI fluctuations, and one much higher, over which zero IR-LDI correlation was assumed. In the simulation, the IR-LDI correlations therefore arise from the lower-layer fluctuations and are reduced by the fluctuations in the upper layer, as well as by thermal noise and finite-aperture filtering. Although the altitude of the higher component is not determined by the data, the data do indicate that the characteristic wind speed of the higher layer must be greater ($\approx$ 10 m/see) than the lower-layer speed of $\approx$ 1 m/see. The simulations which best fit the data suggest that the high-altitude component contributes significantly to the short-period ($\leq$10 seconds) fluctuations, while the long-period (few-minute) fluctuations are predominantly caused by the lower layer. While the simulation accounted for many features of the data, there are systematic features, some of which may be instrumental in origin, which will require further data acquisition and analysis. Errors in the estimate of the lower-layer altitude, which are given in subsection 5b, are based on an assessment of the inadequacy of the current model to completely explain all aspects of the data. The next section describes the Kolmogorov-Taylor modeling and simulations.

4. Modeling and Simulating Atmospheric Fluctuations

The focus of this section is to provide a quantitative model of the path length fluctuations and to use that model to simulate the observed IR-LDI correlation as a function of turbulent atmospheric height, as well as the statistical characteristics of the IR and LDI phase fluctuation time series. A simple, single-layer correlation as a function of turbulent height will be analytically calculated, and then the complications of an additional high-altitude turbulent layer, data editing, thermal noise, and finite-aperture filtering will be considered in a simulation,

4.1. Calculating the Single-Layer IR-LDI Correlation

In this subsection, the single-layer IR-LDI correlation will be calculated as a function of altitude of the layer, ignoring the multilayer, instrumental, and analysis effects to be considered in the next subsection on simulations. The total interferometric IR path length, $\tau_{IR}(\theta, \phi, t)$, due to non-zero tropospheric refractivity, at elevation angle O, azimuth ϕ relative to the orientation of the 1S1 trailers, and at time t is given by

$$\tau_{IR}(\theta, \phi, t) = \tau_{atm}(\theta, \phi, t) + \tau_{LDI}(t) \tag{1}$$

where $\tau_{atm}(0, \phi, t)$ is the contribution to the interferometric path delay from the differences in atmospheric refractivity along the electromagnetic paths from the observed object to each of the two telescopes of the 1S1, and $\tau_{LDI}(t)$ is the ground-based, telescope-differenced LDI path delay due to non-zero refractivity within the telescopes.

For a single turbulent layer, the atmospheric and LDI path delay terms in Equation 1 can be written as

$$\begin{aligned} \tau_{atm}(\theta, \phi, t) &= \frac{1}{c \sin\theta} \int_0^h [\chi(\vec{r}_{2,atm}(\theta, \phi, z), t) - \chi(\vec{r}_{1,atm}(\theta, \phi, z), t)] dz \\ \tau_{LDI}(t) &= \frac{1}{c} \int_0^l [\chi(\vec{r}_{2,LDI}(x), t) - \chi(\vec{r}_{1,LDI}(x), t)] dx \end{aligned} \tag{2}$$

where $\chi(\vec{r}_{i,atm}, t)$ is the refractivity at the point denoted by the vector $\vec{r}_{i,atm}$ along the line of sight at height z above the i^{th} telescope, at time t. The LDI path lengths are defined to lie along the x-axis, For the LDI delay, $\chi(\vec{r}_{i,LDI}(x), t)$ is the refractivity at the vector position a distance x along the LDI path for the i^{th} telescope, at time t. In Equation 2, h is the height of the turbulent atmosphere, the primary parameter to be inferred from the data, 1 is the length of the LDI path, which is about 11 meters[2], and c is the speed of light in vacuum. Using these expressions, the IR-LDI correlation ρ is

$$\rho(\theta, \phi, t) = \frac{< \tau_{IR}(\theta, \phi, t)\, \tau_{LDI}(t) >}{\sqrt{< \tau_{IR}^2(\theta, \phi, t) >< \tau_{LDI}^2(t) >}} = \frac{< \tau_{atm} \tau_{LDI} > + < \tau_{LDI}^2 >}{\sqrt{< \tau_{IR}^2 >< \tau_{LDI}^2 >}} \tag{3}$$

where <> means ensemble average, and the angle and time arguments are understood in the term on the right.

In order to evaluate the correlation, the formalism of Treuhaft and Lanyi (1987) will be used. Using Equation (2) in Equation (3) gives rise to terms like

$$\int_0^l \int_0^h < \chi(\vec{r}_{i,atm}(\theta, \phi, z), t) \chi(\vec{r}_{i,LDI}(x'), t') > dz\, dx'$$

[2]The expression for τ_{LDI} in Equation 2 is somewhat schematic, because the fluctuations along the path from the flat mirror to the parabola are identical to those along the reverse path from the parabola back to the flat mirror. In actual calculations, l is taken to be 5.5 m, and the integral is then multiplied by 2.

The ensemble average can be written in terms of a Kolmogorov refractivity structure function, D_χ:

$$< \chi(\vec{r}_{i,atm}(\theta,\phi,z),t)\chi(\vec{r}_{i,LDI}(x'),t') > \;=\; < \chi^2 > -\frac{1}{2}D_\chi(r = |\vec{r}_{i,atm} - \vec{r}_{i,LDI} - \vec{v}(t-t')|) \tag{4}$$

$$D_\chi(r) \equiv < (\chi(\vec{R} + \vec{r}) - \chi(\vec{R}))^2 >= \frac{C^2 r^{2/3}}{1 + (\frac{r}{L})^{2/3}}$$

where L is a saturation scale modifying the standard 2/3 power law Kolmogorov structure function, and $\dot{R}$ is an arbitrary point in the atmosphere or along the LDI paths. In Equation (4), the structure constant C', wind vector $\vec{v}$, and mean square refractivity $< \chi^2 >$ are assumed independent of the lateral and vertical coordinates of $\vec{r}_{i,atm}$ or $\vec{r}_{i,LDI}$. Exponential profiles of C and $< \chi^2 >$ in the vertical coordinate do not substantially change the vertical scale results extracted below.

Equations (2) and (4) show that there are 4 model parameters needed to describe a turbulent layer in this formalism: the structure constant C, the wind speed $|\vec{v}|$, the saturation scale L, and the height of the turbulent layer h. The wind direction does not strongly influence statistical results and will always be taken to be 45° to the 1S1 trailers. For a single turbulent layer, ρ of Equation (3) is independent of C, because it appears in the numerator and denominator, and it is independent of $|\vec{v}|$, because both τ_{IR} and τ_{LDI} are evaluated at the same time. The correlation p is also very insensitive to L. For example, only a few-percent change in ρ results for an L variation of an order of magnitude. Although Colavita et al. (1987) have inferred an outer scale of turbulence of about 2 km on Mt. Wilson, more recently Bester et al. (1992) and Buscher et al. (1994) suggest that the outer scale of turbulence is frequently a few tens of meters. The temporal structure function of the LDI data of Figure 2 is consistent wit h a saturation scale of 10 m, which is what we use for L to calculate the single-layer ρ.

The above considerations show that the single-layer p is almost completely determined by the turbulent atmospheric height h. Figure 5 shows the model ρ versus h, for (O, ϕ) = (38°, 00), which are the average elevation and azimuth angles of Alpha Orionis observations at the 1S1. Figure 5 results from an analytic calculation of p based on Equation 3, and does not include white system noise, effects of data editing and cycle slips, beam averaging of the IR signal, or a possible additional high-altitude component. If the data of Figure 4a were free of all of these effects, then the resulting IR-LDI long-term correlation of about 0.45 suggests an approximate 60-m turbulent height, based on Figure 5. In actual 1S1 data, the IR-LDI correlations result from the single-layer mechanism which generated Figure 5, but are somewhat reduced by the above effects, as discussed in section 2. This means that in order to arrive, for example, at an observed long-term correlation of 0.45, the lower-layer turbulent height must be lower than 60 m. The simulation which follows describes the departures from the single-layer mechanism, which were required to model the IR-LDI correlations of Figure 4a and the IR and LDI temporal statistics.

4.2. Simulating 2-Layer Correlations and Fluctuation Statistics

The following effects motivate a2-layer simulation of the ISI data: 1) The IR-LDI correlations of Figure 4a *and* the short- and long-term fluctuation statistics of the IR data cannot be reproduced in a model which considers only a single turbulent layer; 2) cycle slips arising from tropospheric and thermal noise will affect the correlation of the IR-LDI data when they are processed through the analysis route described in section 2; and 3) the 1.65-m diameter of the 1S1 mirrors acts as a low-pass filter for the IR data, but not for the LD1 data, which involves light beams of diameter not larger than 1 cm.

It was found there was no single-layered turbulent atmosphere that could reproduce the observed IR-LDI correlation and the observed short-term fluctuation strength of the IR data. This is because the structure constant C (Equation 4) was determined by the LDI statistics to be about 2.4 x $10^{-7} m^{-1/3}$ and, in the single-layer model, the altitude is determined by the IR-LDI correlation (Figure 5). As mentioned above, the single-layer model would have described the long-period data with a turbulent height of about 60 m. Using the inferred structure constant and altitude in Equations 1-4, it was found that the short-term IR fluctuations resulting from the single-layer model were $\approx$ 50% smaller than those of the data. The trend toward smaller IR-LDI correlations at short times, evident in Figure 4a, also could not be reproduced with a single turbulent layer. An additional high-altitude layer with a higher wind speed was needed to improve the model-data agreement for both the IR fluctuation statistics and the IR-LDI correlation. The simulated temporal statistics of the lower and upper layers which best fit the data will be shown in the next section. In addition to incorporating a 2-layer model, the simulations allowed the inclusion of the effects of cycle slips on the IR data. Although the cycle slips were minimized by the means mentioned in section 2, statistical analyses showed that there were still some cycle slips in the analyzed data, even after they were cut into intervals as described. Processing the simulated data through the same algorithm as the real data accounted for cycle slips and their effect on the IR-LDI correlations. Finally, there is an important instrumental difference in the measurement of the IR and LDI path delays which was included in the simulation: The LDI beams are only one or two cm in diameter, so that very localized fluctuations in refractivity can produce high-frequency variations in the path lengths as the fluctuations move through the beams. The IR beam, however, has a diameter of 1.65 m, and hence averages the very short-term ($\approx$ 1-2 second) fluctuations detected by the LDI beam. The IR-LDI correlation at short time scales will therefore be reduced, and this effect was treated in the simulation by boxcar averaging the path length fluctuations above the telescopes with a 2-second window for the lower component only. The window was chosen to be approximately the mirror diameter over the lower-component wind speed. The window which should be applied to the upper component, given its higher wind speed, is about equal to the sampling interval of the data.

Inclusion of the above effects necessitated a simulation of the 1S1 data, with at least two layers. Simulations were accomplished using the calculated covariance matrices of the IR and LDI time series, including the covariance between the two time series. The techniques of Bierman (1977) were used to transform a general covariance matrix into a diagonal covariance matrix, generate white-noise delays corresponding to the diagonal covariance matrix, then transform those delays back into a time series obeying the general covariance matrix. Terms of the following form were required for the covariance matrix:

$$<\tau_{IR}(\theta,\phi,t)\,\tau_{IR}(\theta,\phi,t')> - <\tau_{IR}(\theta,\phi,t)><\tau_{IR}(\theta,\phi,t')>$$
$$<\tau_{IR}(\theta,\phi,t)\tau_{LDI}(t')> - <\tau_{IR}(\theta,\phi,t)><\tau_{LDI}(t')>$$
$$<\tau_{LDI}(t)\tau_{LDI}(t')> - <\tau_{LDI}(t)><\tau_{LDI}(t')>$$

where t and t' are times within a few-minute scan. They were evaluated with the methods discussed in the last subsection and in Treuhaft and Lanyi (1987).

5. Results and Error Analysis

In this section we first show the level of agreement between the best simulation and the data, and discuss the characteristics of the vertical scales of turbulence suggested by the parameters which generated the best simulation. We then describe potential errors in the values of the parameters used in the best simulation.

5.1. The Simulation-Data Agreement and the Optimal Simulation Parameters

The level of agreement between the best simulation and the data is demonstrated by Figure 6 and Table 1, which show IR-LDI correlations and temporal statistics, respectively. A two-component turbulent atmospheric model, with Gaussian distributions of structure constants for both the lower and upper component, was used to produce the simulation entries of Figure 6 and Table 1. The upper component was assumed to be completely uncorrelated with the lower component and hence with the LDI path delays. The agreement in Figure 6 is better than 20% for time intervals greater than 30 seconds, and of the order of 50% for shorter time scales. The data-simulation agreement in Table 1 is better than 20% for the mean values of the statistics quoted. Some of the simulation statistical standard deviations differ from those of the data by as much as 50'%0. Figures 6a and and 6b suggest that there is some unmodeled physical mechanism causing high-frequency filtering of the IR signals, which in turn causes the loss of correlation at the shorter time scales, and the smaller population of the first bin in Figure 6b. This will be discussed in the next subsection.

The parameters generating the simulation which best agreed with the data are shown in Table 2. The optimal value for the altitude of the lower component, which is responsible for the IR-LDI correlation, was found to be 45 m. This altitude is within a factor of 2-3 of the tree height and other structures near the interferometer and suggests that the lower layer of turbulence may be induced locally, by wind blowing around and through these objects. The structure constant and saturation scale of the lower component were adjusted to produce the observed short- and long-term LDI fluctuations. Although the upper-component altitude and structure constant were adjusted to fit the data, there is no absolute significance to either the vertical scale or structure constant of the upper component taken by themselves. The relevant simulation properties depend approximately on the product of the

upper-component structure constant and the square root of the altitude. The 1 m/see wind speed of the lower component was determined from the LDI data by finding the average temporal lag offset required to maximize the correlation between the LDI path length fluctuations in each of the telescopes. This lag offset, which was found to be about 10 seconds, was interpreted as the time required for an inhomogeneity to move from one telescope to the other, along the baseline, which was about 10 m. The wind speed for the upper component was chosen because it is characteristic of wind speeds aloft. The 1S1 data alone also require a higher wind speed for the upper component, in order to provide the level of observed short-period fluctuation in Table 1 and the short-period decorrelation in Figure 4a. The saturation scale of the upper component was chosen to be much larger than the baseline separation and much larger than that of the lower component, because there seems no reason to assume that the high-altitude saturation scale is small.

Figure 7 shows the structure functions of the simulated average lower and upper components along with the combined structure function. It can be seen that the upper component contributes most of the short-term fluctuation needed for agreement with the data, while the lower component primarily generates the long-term fluctuations in the model data. That a high-altitude atmospheric component dominates short-period fluctuations is consistent with the common observation on Mt. Wilson of rapid star twinkle during locally calm conditions on the ground. The difference in the time-dependence of the lower- and upper-layer structure functions is due to the order-of-magnitude difference in their wind speeds, which is an essential feature of the model. Figure 7 also demonstrates how the statistics of the lower and upper components constrain the model lower-layer altitude. For example, one could postulate a much smaller lower-layer altitude, which would require a larger admixture of the upper-layer turbulence to restore the level of IR-LDI correlation agreement in Figure 6a. But a larger admixture of the upper-layer turbulence would cause the total short-term IR fluctuation to grow, and destroy the data-model agreement of this statistic in Table 1. The improvement in seeing or astrometric accuracy to be gained by calibrating the lower $\approx$ 45-m component can be estimated within the framework of the model. The seeing or astrometric accuracy is a function of the IR rms fluctuation in a scan. If the lower component fluctuations were completely removed by measurement, the simulated IR rms drops from the value in Table 1 to 0.4 cycles, suggesting that lower-component calibration has the potential for reducing the IR rms by about 50%, with a corresponding improvement in astrometric accuracy. The error on this assessment is described in the next subsection with the errors on the parameter estimates.

5.2. Parameter Error Analysis

In order to interpret the degree to which the extracted parameters reflect the actual vertical scales at Mt. Wilson, i.e. in order to determine the error on the derived parameters in Table 2, two classes of parameter error should be considered: 1) the range of parameter values about the best-fit values, which results from the modeled statistical variations in the data and 2) systematic errors caused by model inadequacies which affect estimated parameters. In order to assess the importance of the first type of error, deviations from the values of the parameters in the tables were tried, and it was found that they caused significantly worse agreement with the data if the excursions were bigger than about

20%. The parameter errors due to the second mechanism cited above were of the same order. The unmodeled short-period filtering suggested by Figure 6a and 6b represents the most obvious potential model inadequacy. That is, the simulation-data agreement in Figure 6 improves if preaveraging times in excess of those warranted by finite-aperture filtering are applied to the simulation data. This model inadequacy, which is probably due to an incomplete description of the turbulence in the ground-based paths, may be causing up to a 30% error in the inferred lower-component height. It is possible, for example, that wind speeds along the path between the mirrors are slower than those perpendicular to it, necessitating longer preaveraging times for finite-aperture effects, or that the temporal spectrum of fluctuations is different near the ground, due to the aerodynamic effects of the 1S1 trailers. It is also possible that there are other unmodeled instrumental effects causing the high-frequency filtering of the IR or LDI signals. Since we could not verify which, if any, of these mechanisms causes the short-period filtering, we did not apply any preaveraging over ad hoc time scales to the results of Figure 6a and 6b. Additional simulations with a range of preaveraging time scales, which produced better data-simulation agreement than that of Figure 6, changed the estimated altitude of the lower turbulent layer by about 15 m; we therefore take 15 m to be the level of systematic error in the lower component altitude. The systematic error in the other adjusted parameters in Table 2, due primarily to incorrect physical modeling inputs, is gauged to be about 30%. The level of astrometric improvement due to lower-component calibration, assigned a model value of 50% above, should more conservatively be assigned a value of 30-50%, based on the simulations with different preaveraging times. Methods for reducing the levels of systematic errors will be discussed in the next section.

6. Summary, Analysis Improvements, and Future Plans

The 1S1 IR and LDI 1992-93 path length fluctuation data are modeled as arising from a lower- and upper-component of Kolmogorov-Taylor atmospheric turbulence with finite outer scales. A single-layered model cannot simultaneously account for the observed IR-LDI correlation and the temporal statistics of the IR and LDI time series. The altitude of the lower component which generates the best fit to the observed IR-LDI correlation and the temporal statistics of the IR and LDI time series taken separately, was about 45 m with a systematic error of about 15 m. It is possible that trees or other structures near the 1S1 are in part responsible for locally generating the lower component of turbulence. This lower-layer altitude is consistent with qualitative arguments based on the outer scale of a few tens of meters observed in the horizontal direction. In the best-fit model, the upper-component contributes primarily to the short-term (< 10 seconds) IR fluctuations, while the lower component dominates the longer-period fluctuations. Effects of white thermal noise, data editing, and instrumental spatio-temporal filtering were included in the simulation. Possible mismodeling of near-ground refractivity fluctuations, suggested by poorer simulation-data agreement at short time scales, is largely responsible for the quoted systematic error. The results of this paper suggest that calibration of the lower component could improve the interferometric phase accuracy by about 30-50%.

Both improvements in modeling and the acquisition of new data types on Mt. Wilson would help to more accurately assess the vertical scales of turbulence. As mentioned in the text, a more

precise description of the high-frequency fluctuations near the ground might improve the short-period model-data agreement. Other modeling improvements include introducing correlations between the lower and upper components of turbulence. In the present study, the correlation between the two components was assumed to be zero. Allowing the wind vector to be a continuous, possibly stochastic, function of altitude would be more realistic and might improve the data-simulation agreement of Figure 6 and Table 1. Allowing the structure constant and saturation scales to vary continuously as a function of altitude would also be more realistic, but altitude profiling of these parameters is probably beyond the scope of what can be uniquely inferred from 1S1 data as they are currently taken,

Beyond additional modeling, measurements aimed at directly detecting vertical profiles of turbulence during interferometric observations would be extremely useful. Simultaneous high-speed temperature and barometric profiling of the atmosphere with the first few tens of meters above the 1S1 would substantially supplement the approach taken in this paper, Another possibility for improving the determination of vertical scales of turbulence is to make LDI measurements along vertical paths near the interferometer. Additional LDI measurements are a possible option for measuring the strength of fluctuations originating at low altitudes

This work represents one phase of research carried out at the Jet Propulsion Laboratory, California Institute of Technology, under contract with the National Aeronautics and Space Administration. The University of California portion of the work was supported by grants from the United States Office of the Chief of Naval Research (NOO01489-J-1583) and the National Science Foundation (AST-91 19317). We would like to thank G.G. Degiacomi and D. D. Hale for help with the observations.

STATISTIC	DATA Mean, Standard Deviation (IR Cycles)	SIMULATION Mean, Standard Deviation (IR Cycles)
IR RMS Fluctuation	*1,024, 0.562*	*0.998, 0.373*
LDI RMS Fluctuation	*0.252, 0.046*	*0.266, 0.096*
IR point-to-point RMS	*0.145, 0.024*	*0.160, 0.035*
LDI point-to-point RMS	0.049, *0.009*	*0.052, 0.018*

Table 1: Statistics from the 1S1 Alpha Orionis data taken in 1992-3 and those from a Kolmogorov-Taylor, two-component simulation with lower and upper atmospheric component characteristics as in Table 2. The first two entries are rms scatters about linear fits over few-minute scans, while the last two are rms differences in adjacent time series points, separated by 0.3 seconds on average.

PARAMETER	LOWER Mean Value Standard Deviation	UPPER Mean Value Standard Deviation
Altitude (m)	45	1000"
Structure Constant (x $10^{-7}m^{-1/3}$)	2.42, 0.85	0.08:0.04
Wind Speed (m/see)	1	10
Saturation Scale (m)	10	1000

Table 2: Parameters generating the simulated turbulence for lower and upper atmospheric components.

"Note that the altitude and structure constant of the upper layer are not separately determinable. The relevant simulation properties depend on the product, structure constant x $\sqrt{(\text{altitude})}$.

REFERENCES

Bester, M., Danchi, W. C., Degiacomi, C. G., Greenhill, L. J., and Townes, C. H. 1992, ApJ, 392, 357

Bierman, G. J. 1977, Factorization Methods for Discrete Sequential Estimation, (Orlando, FL: Academic Press)

Buscher, D. F., Armstrong, J. T., Hummel, C. A., Quirrenbach, A., Mozurkewich, D., Johnston, K. J., and Denisen, C. S. 1994, submitted to Appl. Optics

Colavita, M. M., Shao, M., and Staelin, D. H. 1987, Appl. Optics, 26, 4106

Treuhaft, R. N. and Lanyi, G. E. 1987, Radio Science, 22, 251

This preprint was prepared with the AAS LaTeX macros v3.0.

Fig. 1.— A single 1S1 trailer showing the flat mirror (right), the focusing parabola (left), and the helium-neon laser distance interferometer beams (dashed lines). The beams used to calibrate path length fluctuations within the instrument, called "LDI" in the text, are those centrally located on the flat and the parabola.

Fig. 2.- An IR-LDItime series from anobservation of Alpha Orionis, taken on8Septemberl992.

Fig. 3.— Histogram of the point-to-point phase change for the IR data of Figure 2. The points are separated by 0.2 seconds,

Fig. 4.— a) The IR-LDI correlation for all Alpha Orionis 1992-3 dataversus time interval over which the correlation was taken. The baseline length was 10m. b) Histogram of the intervals used for correlation evaluation in Figure 4a from all the 1992-3 Alpha Orionis ISI data.

Fig. 5.— Calculated IR-LDI correlation, for a single-turbulent-layer model, as a function of atmospheric height for elevation and azimuth of 38 degrees and O degrees respectively.

Fig. 6,— a) Simulated and real IR-LDI correlation, with the simulated data generated from turbulent heights of 45 and 1000 meters, with wind speeds of 1 m/see and 10 m/see, respectively, with the structure constants as noted in table 2. The last data point represents only one interval and therefore is shown with no error bar. b) Histogram for the simulated IR-LDI correlation of Figure 6a, generated with 45-m and 1000-m turbulent heights. The asterisks are the histogram for the 1992-3 1S1 data, normalized to the second bin of the simulated data.

Fig. 7.— Simulated IR structure functions of time for lower, upper, and combined turbulent atmospheric components.

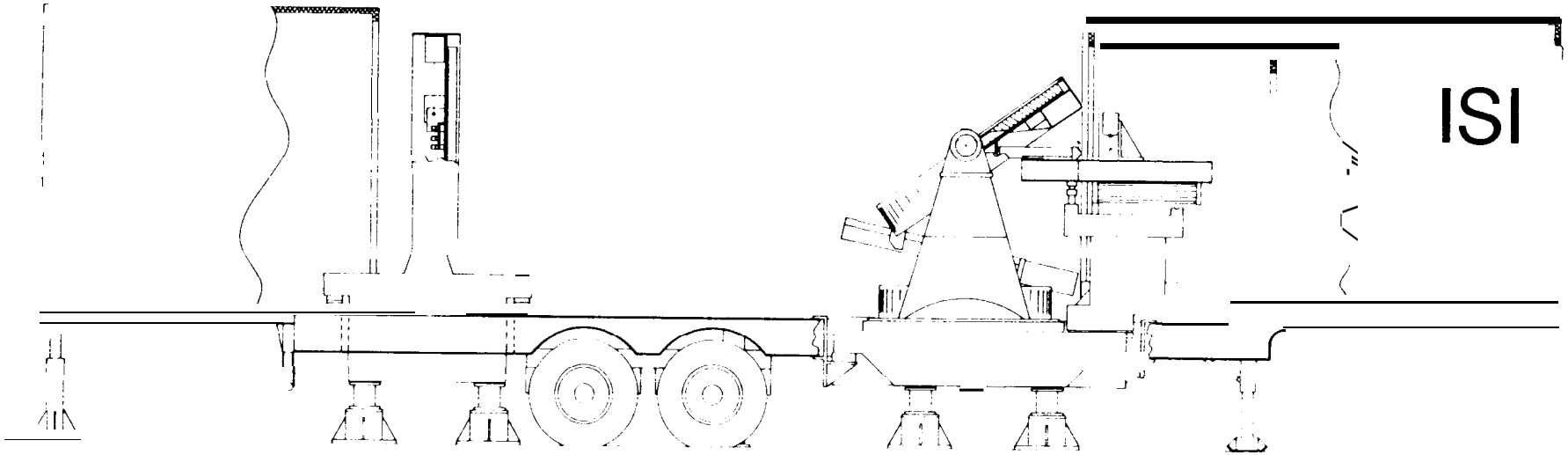

UCB INFRARED SPATIAL INTERFEROMETER

1 METER

SEMI-TRAILER OUTLINE

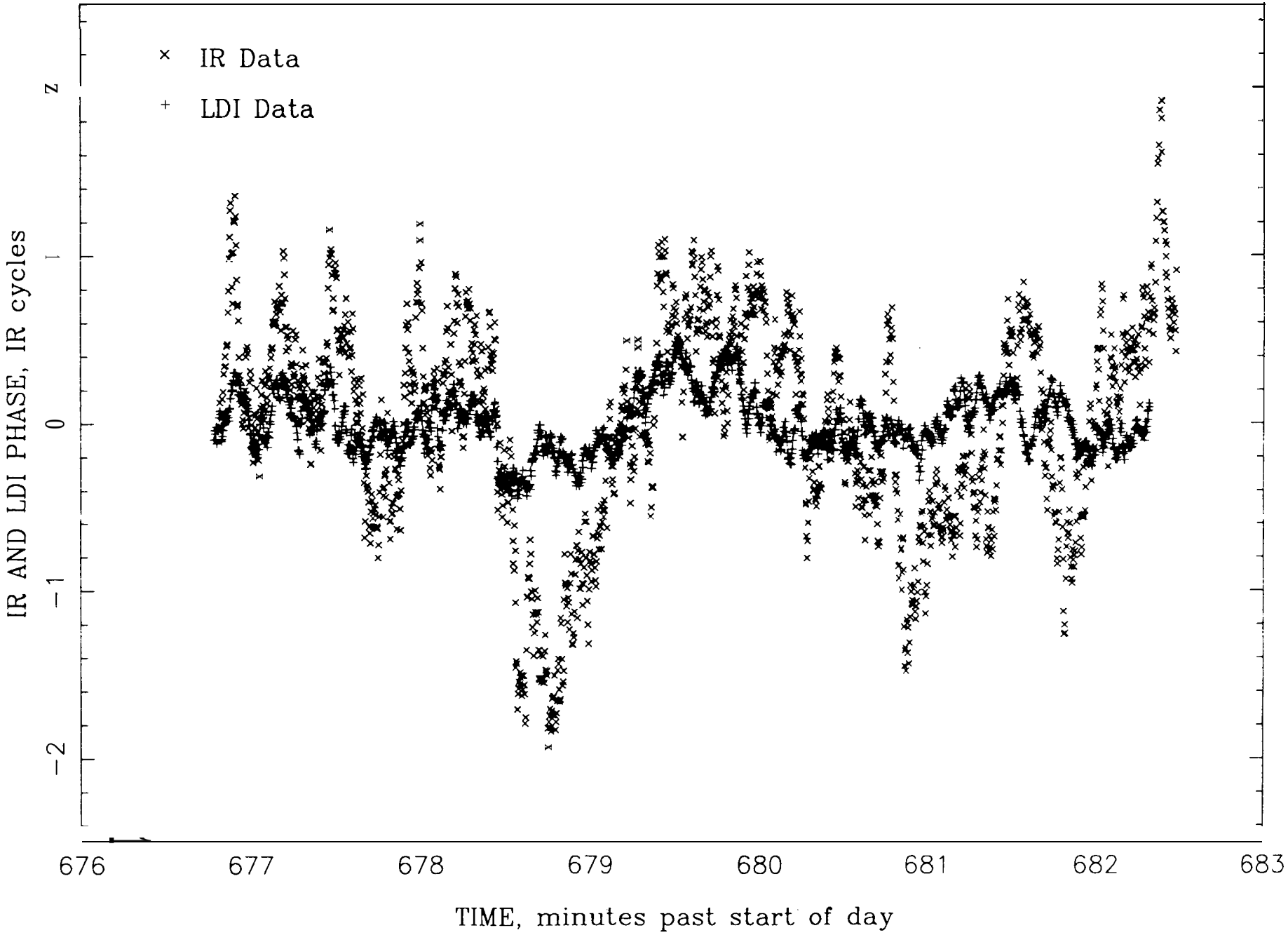
× IR Data
+ LDI Data
IR AND LDI PHASE, IR cycles
2
1
0
−1
−2
676
677
678
679
680
681
682
683
TIME, minutes past start of day

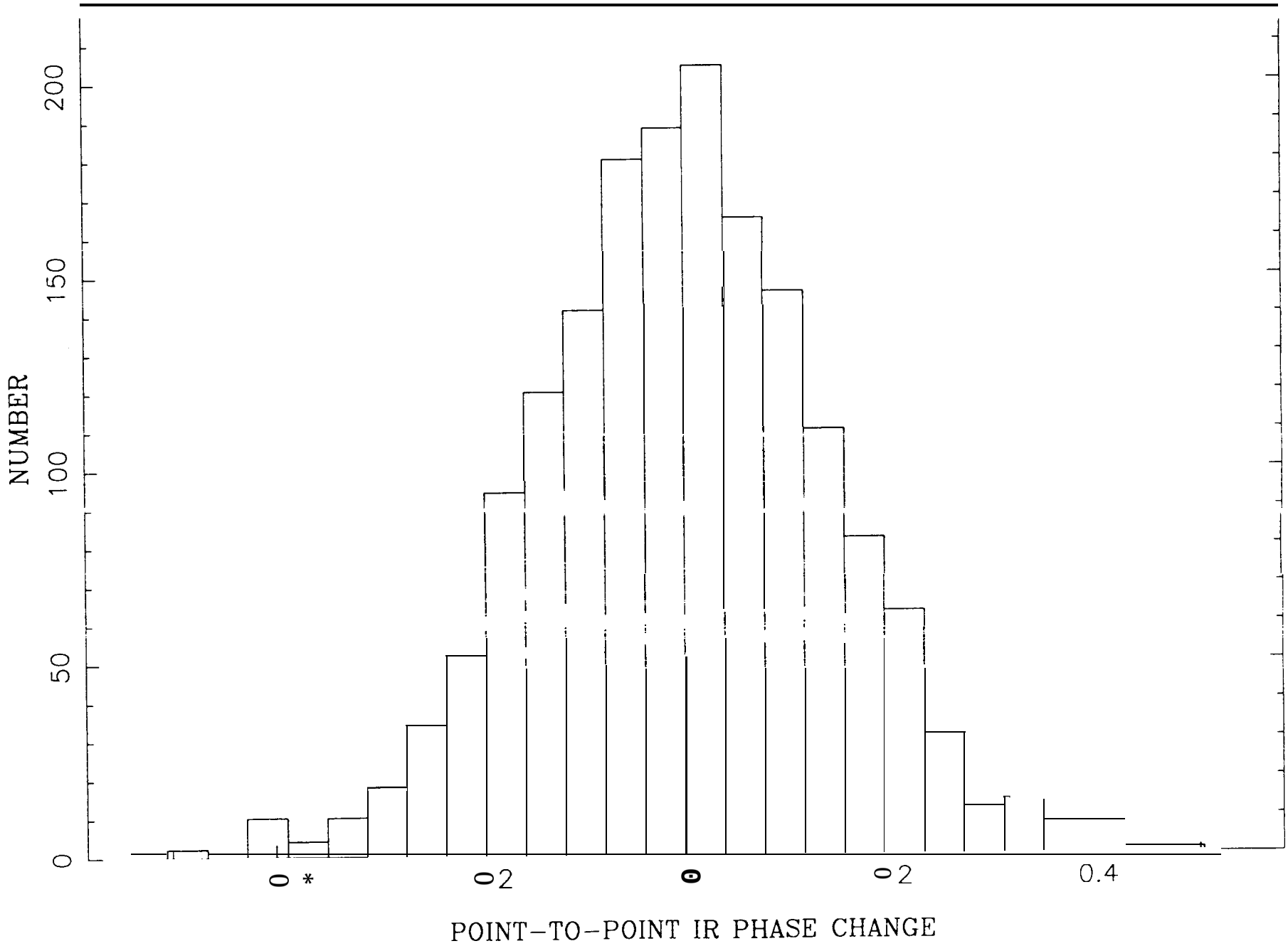
NUMBER
0
50
100
150
200
0 *
02
0
02
0.4
POINT-TO-POINT IR PHASE CHANGE

IR–LDI CORRELATION
0.2
0.3
0.4
0.5
TIME NTERVAL, seconds
20
60
80
100

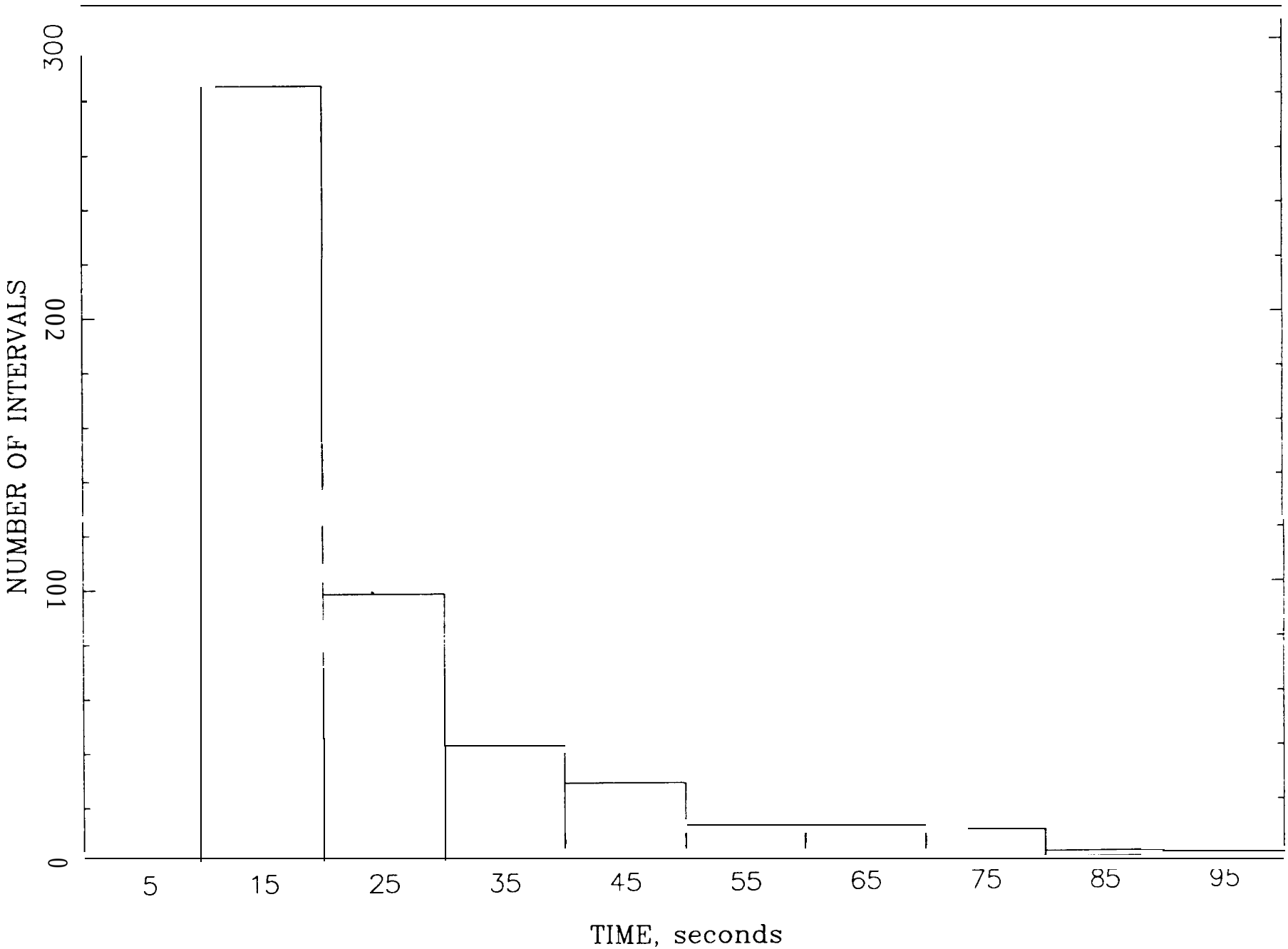
NUMBER OF INTERVALS
0
100
200
300
5
15
25
35
45
55
65
75
85
95
TIME, seconds

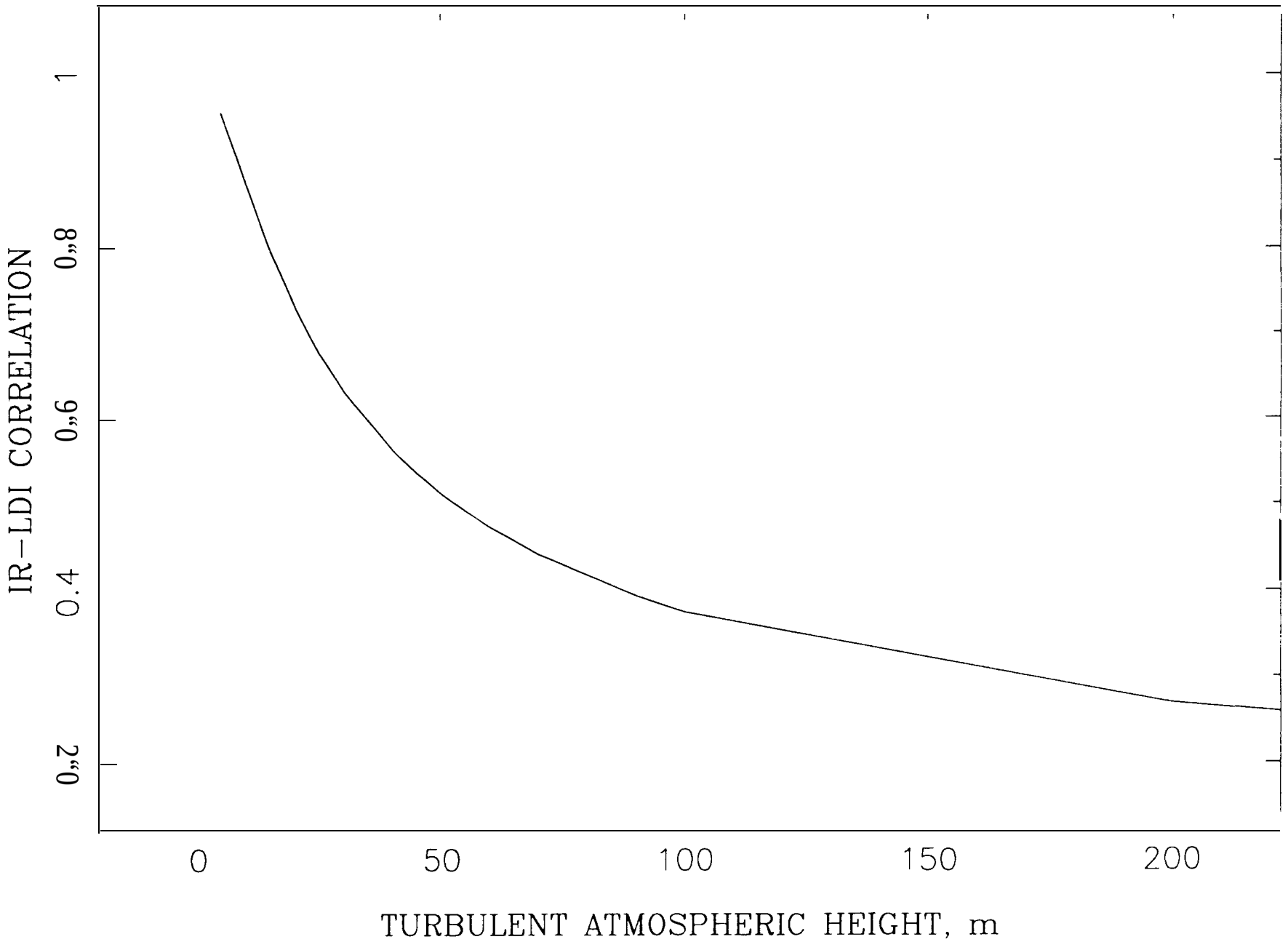
IR–LDI CORRELATION
0,2
0.4
0,6
0,8
1
0
50
100
150
200
TURBULENT ATMOSPHERIC HEIGHT, m

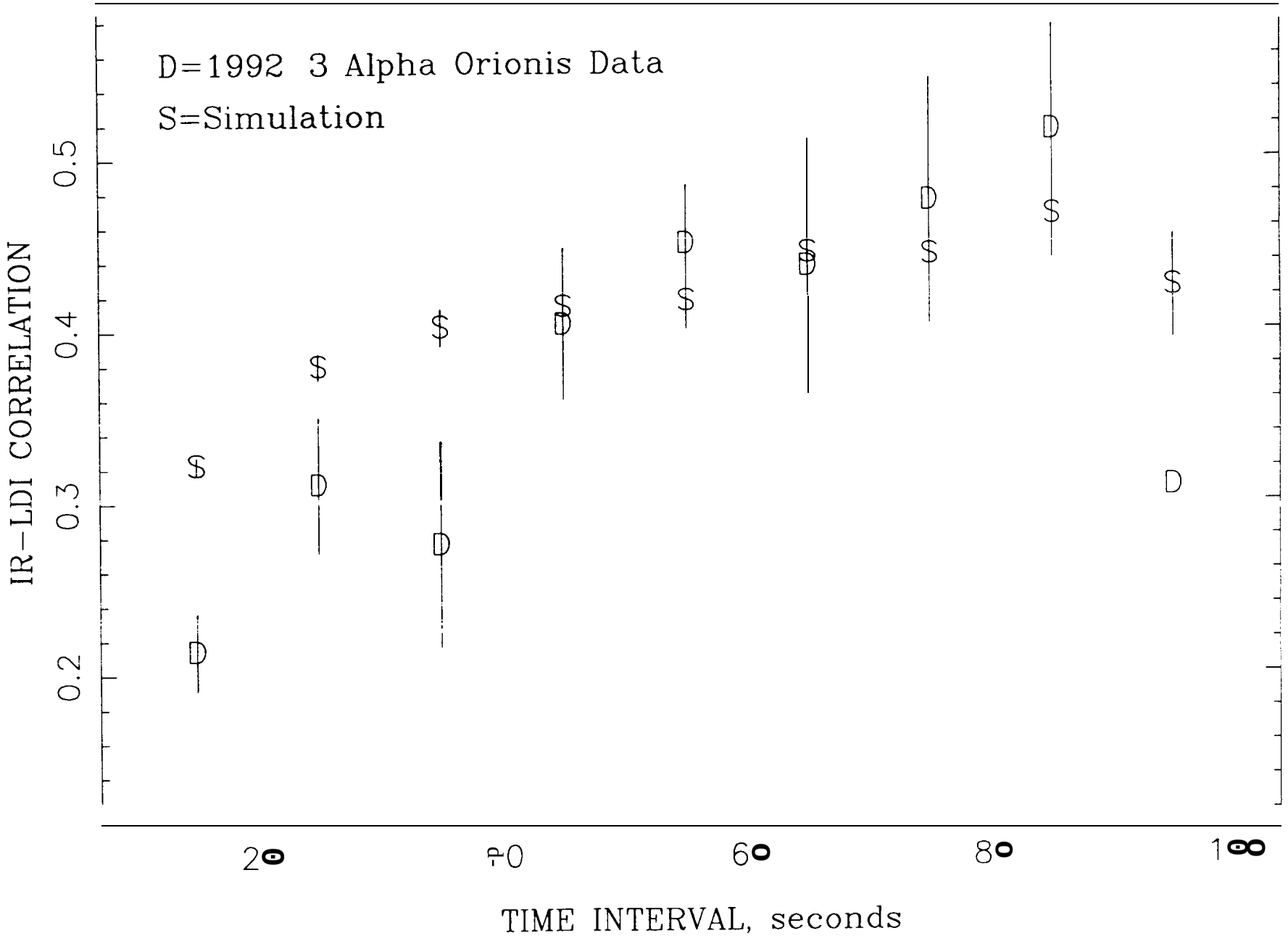
D=1992 3 Alpha Orionis Data
S=Simulation
IR-LDI CORRELATION
0.2
0.3
0.4
0.5
20
40
60
80
100
TIME INTERVAL, seconds

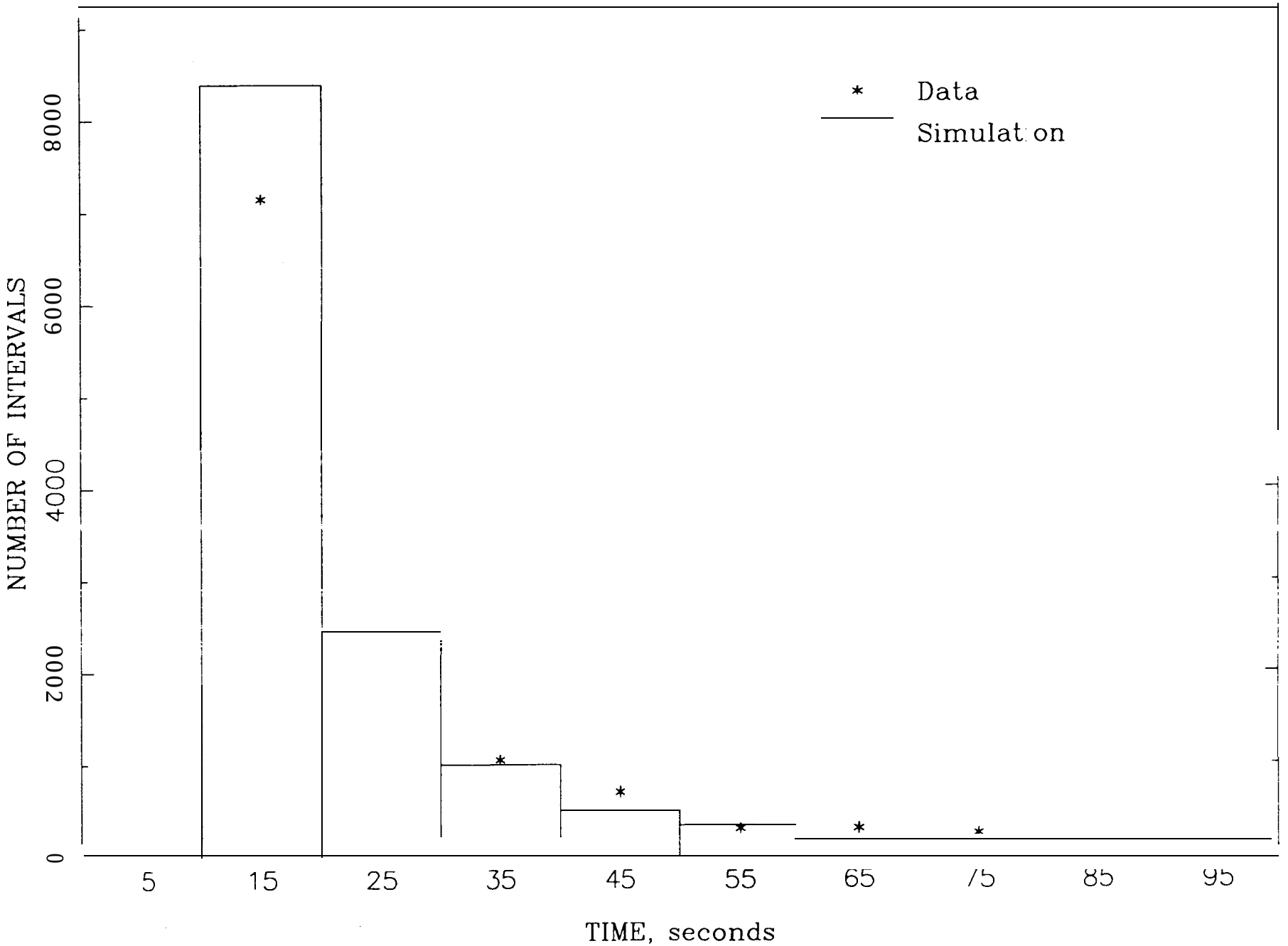
NUMBER OF INTERVALS
0
2000
4000
6000
8000
5
15
25
35
45
55
65
75
85
95
TIME, seconds
Data
Simulation

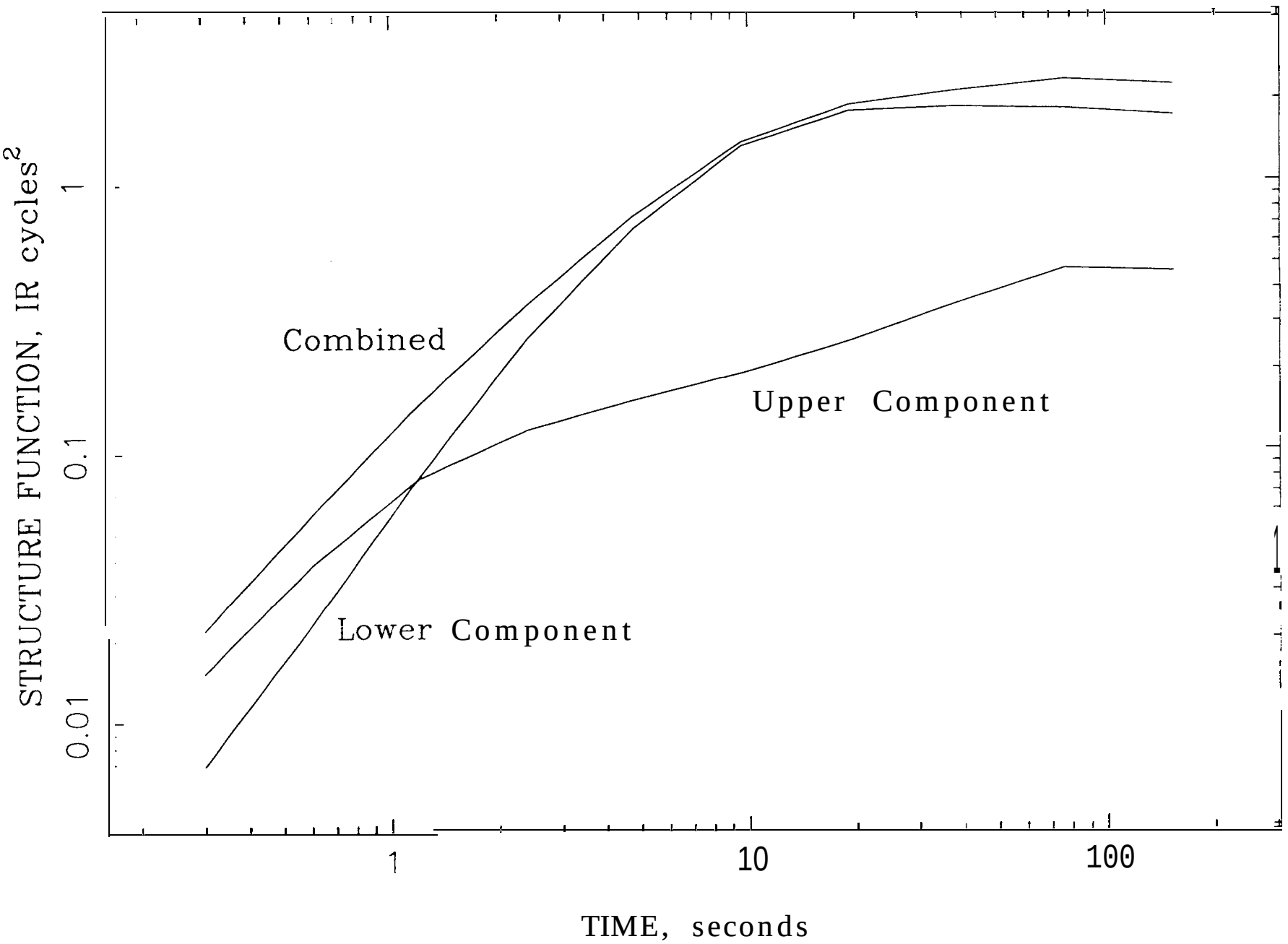
STRUCTURE FUNCTION, IR cycles^2
1
0.1
0.01
Combined
Upper Component
Lower Component
1
10
100
TIME, seconds